Optimal heterogeneity of a highly renewable pan-European electricity system

Emil H. Eriksen[a], Martin Greiner[b,c]

[a] *Department of Physics and Astronomy, Aarhus University, 8000 Aarhus C, Denmark*
[b] *Department of Mathematics, Aarhus University, 8000 Aarhus C, Denmark*
[c] *Department of Engineering, Aarhus University, 8200 Aarhus, Denmark*

Abstract

The resource quality and the temporal production pattern of variable renewable energy sources varies significantly across Europe. A homogeneous distribution of wind and solar capacities makes inefficient use of the resources, resulting in high system costs. A heterogeneous redistribution of renewable assets maximising the overall capacity factor results in smaller investments in renewable capacities, but higher costs of transmission. The cuckoo search algorithm is used to find optimal distributions of production capacities minimising backup, transmission and renewable capacity costs simultaneously, resulting in lower costs of electricity.

Keywords: renewable energy system, levelised cost of electricity, wind power generation, solar power generation, cuckoo search

1. Introduction

The ambitious renewable targets set by the European leaders[1] imply that the renewable penetration will increase significantly in the years to come.

[TALK ABOUT ELECTRIFICATION HERE [2, 3]]

At present, the leading renewable technologies are wind, solar PV and hydro, of which only wind and solar PV have potential for large-scale expansion. For this reason, the analysis will consider only wind and solar PV explicitly. Since wind and solar PV are both variable renewable energy resources (VRES), backup generation is needed if power outages are to be avoided. Backup generation equals additional system cost and must thus be kept at a minimum.

The backup requirements depends on the mismatch between load and VRES generation. Using the degrees of freedom associated with the choice of VRES layout, it is possible to shape the temporal pattern towards the load pattern so that the mismatch, and thus the backup requirements, is lowered. It is possible to reduce the VRES layout is reduced to a single parameter, the mixing parameter, by assuming a homogeneous mix between wind and solar PV across all countries, and that all countries install enough VRES capacities to cover their load on average. This approatch is demonstrated e.g. in [7, 8] where balancing and storage optimal mixes are found.

Further reductions in backup requirements are possible by exchanging energy between the countries through a transmission network [4, 5]. Other relevant papers on the advantages and costs of grid extensions are [14, 15].

Email addresses: emilhe@phys.au.dk (Emil H. Eriksen), greiner@eng.au.dk (Martin Greiner)

In a conventional energy system, the siting of production capacities is not a concern. No geographical areas are preferable, so the power plants are simply put where the demand is present. For VRES, the situation is more complicated. The primary reason is the geographical variation of the VRES quality. The resource quality is quantified through the capacity factor ν defined as

$$\nu = \frac{\text{Average production}}{\text{Rated capacity}}. \tag{1}$$

The capacity factor is a number between 0 and 1, where 0 means no production and 1 means maximum production at all times. Capacity factors for the European countries for onshore wind, offshore wind and solar PV are listed in table 1. The capacity factors were calculated using the Renewable Energy Atlas[6] (REA). The VRES layout at country level was chosen as a homogeneous distribution across the 50% best sites. For wind conversion, the power curve of the Vestas V90 3.0MW turbine was assumed. For solar conversion, the Scheuten P6-54 solar PV panel oriented south and tiled from horizontal to a degree equal to the latitude of installation was applied.

The secondary reason the geographical variation of the temporal production pattern of VRES. For Europe, this effect is particularly important for wind since Europe is large compared to the wind correlation length of ≈ 1000 km [17].

With these points in mind, allocating resources in proportion to the mean load of a country and an overall fixed mixing factor does not seem ideal. In this paper, the homogeneous assumption is lifted. Different approaches to cope with the resulting large number of degrees of freedom are considered ranging from heuristic layouts constructed from resource quality knowledge to layouts obtained through

numerical optimization. The objective is to find heterogeneous layouts with properties superior to the homogeneous layouts, in particular a lower cost of electricity.

This paper is organised as follows: Section 2 discusses the general modelling of the electricity system, the key metrics and the construction of heterogeneous layouts. In section 3 the performance of the different layouts and the resulting renewable penetrations for individual European countries are discussed. Section 4 contains an analysis of the sensitivity of the results to reductions in solar costs and to expansions in offshore wind capacities. We conclude the paper with a discussion on the results and an outlook on future research.

2. Methods

2.1. The electricity network

The European electricity network is modelled using a 30-node model where each node represents a country. The nodal load is determined from historical data, while wind and solar production data are calculated using a combination of weather data and physical models[6]. Initially, wind is assumed to be onshore only. For each node n the generation from VRES,

$$G_n^R(t) = G_n^W + G_n^S, \tag{2}$$

can be expressed through two parameters. The penetration γ determines the amount of energy generated relative to the mean load of the node,

$$\langle G_n^R \rangle = \gamma_n \langle L_n \rangle, \tag{3}$$

while the mixing parameter α fixes the ratio between wind and solar,

$$\langle G^W \rangle = \langle G_n^R \rangle \alpha_n, \tag{4}$$

$$\langle G^S \rangle = \langle G_n^R \rangle (1 - \alpha_n). \tag{5}$$

The nodal difference between VRES generation and load

$$\Delta_n(t) = G_n^R(t) - L_n(t) \tag{6}$$

is called the mismatch. To avoid power outages, the demand must be matched at all times. Since storage is not considered, any power deficits must be covered by backup generation. Dispatchable resources are not modelled explicitly, but are considered a part of the backup generation. If $\Delta_n(t) \geq 0$, excess energy can be curtailed $C_n(t)$, while if $\Delta_n(t) < 0$ backup generation $G_n^B(t)$ is needed.

$$C_n(t) = +\max(\Delta_n(t), 0) \tag{7}$$

$$G_n^B(t) = -\min(\Delta_n(t), 0) \tag{8}$$

Summing the two terms, we get the nodal balancing $B_n(t) = C_n(t) + G_n^B(t)$. It is possible to lower the balancing needs by transmission. Nodes with excess production export energy $E_n(t)$, allowing nodes with an energy deficit to import energy $I_n(t)$ to (partly) cover their energy deficit. The nodal injection, $E_n(t) - I_n(t)$, is denoted $P_n(t)$. This leads to the nodal balancing equation,

$$G_n^R(t) - L_n(t) = B_n(t) + P_n(t). \tag{9}$$

The vector of nodal injections $\mathbf{P}$ is called the injection pattern. The actual imports and exports, and thus the injection pattern, depend on the business rules of the nodal interactions. It is convenient to express business rules in terms of a two step optimization problem. The top priority is to minimize the backup generation,

$$\begin{aligned} \text{Step 1:} \quad & \min_{\mathbf{P}} \quad \sum_n G_n^B = G_{min}^B \\ & \text{s.t.} \quad f_l^- \leq f_l \leq f_l^+ \end{aligned} \tag{10}$$

where $f_l^{\pm}$ denote any flow constraints on the network. The minimal backup energy can be realized by a number of injection patterns. The degeneracy is removed by choosing the injection pattern that minimizes the sum of squared flows,

$$\begin{aligned} \text{Step 2:} \quad & \min_{\mathbf{P}} \quad \sum_l f_l^2 \\ & \text{s.t.} \quad f_l^- \leq f_l \leq f_l^+ \\ & \text{s.t.} \quad \sum_n G_n^B = G_{min}^B. \end{aligned} \tag{11}$$

The purpose of the second minimization step is twofold. First, it ensures that the nodes exchange energy in the most localized way. Secondly, it guarantees that the solution resembles a physical flow[9].

2.2. Key metrics

Inspired by [10], the energy system cost is calculated based on a few key parameters. Besides the cost of the VRES capacities, $\mathcal{K}^{\mathcal{W}}$ and $\mathcal{K}^{\mathcal{S}}$, costs for the backup system and the transmission network are included. The backup system cost is split into two components, the cost of backup capacity $\mathcal{K}^B$ (including maintance) and the cost of backup energy E^B. The backup capacity cost covers expenses related to keeping the power plants online while the backup energy cost accounts for the actual fuel cost. Expressed in units of the average yearly load, the backup energy is given by

$$E^B = \frac{\sum_n \sum_t G_n^B(t)}{\sum_n \sum_t L_n(t)} = \sum_n \frac{\langle G_n^B \rangle}{\langle L_n \rangle}. \tag{12}$$

In principle, the backup capacity is fixed by a single extreme event. However with this definition, the results will be highly coupled to the particular data set used. To decrease the coupling, the 99% quantile is used rather than the maximum value,

$$q_n = \int_0^{K_n^B} p_n(B_n) dB_n \tag{13}$$

where $p_n(B_n)$ is the time sampled distribution of backup power and $q_n = 0.99$. With this choice, the backup system will be able to cover the demand 99% of the time. The remaining 1% is assumed to be cover by unmodeled system components like storages or demand side management. In accordance, the transmission capacity $\mathcal{K}^T$ is defined so that the demand is met 99% of the time. Since transmission can be positive and negative, the larger of the absolute value of the 0.5% and the 99.5% quantile is used rather than the 99% quantile,

$$\mathcal{K}^T = \sum_l \mathcal{K}_l^T \tag{14}$$

with

$$\mathcal{K}_l^T = \max\{-Q_{0.5\%}, Q_{99\%}\} \tag{15}$$

and

$$x = \int_{-\infty}^{Q_x} p_n(f_l) dF_l. \tag{16}$$

Cost assumptions for the elements of an energy system vary greatly across the literature [10]. In this study, the cost assumption published by [11] have been adapted, see table 2. The cost assumptions are in the low end for VRES which reflects the expectation that the cost of VRES will go down in the future as the penetration increases [12].

Table 2: Cost assumptions for different assets.

Asset	CapEx [€/W]	Fixed OpEx [€/kW/y]	Variable OpEx [€/MWh]
CCGT	0.9	4.5	56.0
Solar PV	1.5	8.5	0.0
Offshore wind	2.0	55.0	0.0
Onshore wind	1.0	15.0	0.0

From the VRES penetration, the mixing factor and the mean load, the effective production of each node can be calculated. Dividing by the associated capacity factor, one arrives at the capacity. Except for transmission capacity, the present value of each element can be calculated directly as

$$V = \text{CapEx} + \sum_t \frac{\text{OpEx}_t}{(1+r)^t} \tag{17}$$

where r is the return rate assumed to be 4%. The transmission capacity cannot be translated directly into cost as the cost depends on the length and the type of the link. Link lengths have been estimated as the distance between the country capitals. Link costs are assumed to be 400€ per km for AC links and 1,500€ per km for HVDC links. For HVDC links, an additional cost of 150,000€ per converter station (one in each end) is added [13–15]. The layout of AC and DC links has been constructed by [4] from ENTSO-E data.

Given the element costs, the system cost V_{sys} is calculated by summation. To allow for comparison of different energy systems, the levelised cost of electricity (LCOE) is a convenient measure. The LCOE is the cost that every unit of energy produced during the lifetime of the project must have to match the present value of investment [16],

$$\text{LCOE} = \frac{V_{sys}}{\sum_t \frac{L_{EU,t}}{(1+r)^t}}. \tag{18}$$

See [10] for more details on the cost calculation.

2.3. Heuristic layouts

The simplest way to distribute the renewable resources would be to assign the resources homogeneously (relative to the mean load of the node) so that $\gamma_n = \gamma$ (and $\alpha_n = \alpha$). However this assignment might not be ideal since the capacity factors vary significantly between the nodes. Having this point in mind, an intuitive way to proceed would be to assign resources proportional to the resource quality. To generalise the idea, the resource quality expressed through ν is raised to an exponent β as suggested by [11]. For a wind only layout, the γ values are given by

$$\gamma_n^W = \left(\nu_n^W\right)^\beta \frac{\langle L_{EU}\rangle}{\sum_m \langle L_m\rangle \left(\nu_m^W\right)^\beta}. \tag{19}$$

An equivalent expression for the solar only layout is obtained by the substitution $W \to S$. Examples for $\beta = 1$ are shown in figure 1. In the layout illustrations, each bar represents a country n. The height of the bar is γ_n while the mix α_n between onshore wind (dark blue) and solar (yellow) is expressed through the bar colouring. β layouts for any value of α can be expressed as a linear combination of the wind and solar only layouts with

$$\gamma_n = \alpha\gamma_n^W + (1-\alpha)\gamma_n^S \tag{20}$$

and

$$\alpha_n = \frac{\alpha\gamma_n^W}{\alpha\gamma_n^W + (1-\alpha)\gamma_n^S}. \tag{21}$$

For practical reasons, it is not possible to realise arbitrarily heterogeneous layouts. To constrain heterogeneity, the heterogeneity factor K is introduced by requiring

$$\frac{1}{\text{K}} \leq \gamma_n \leq \text{K}. \tag{22}$$

With this definition, K = 1 corresponds to a homogeneous layout (in terms of γ) while K = ∞ represents unconstrained heterogeneity.

Although the capacity factor of a β layout is higher than the capacity factor of the homogeneous layout (for $\beta > 0$), it is possible to achieve an even higher capacity factor without violating the constraints in equation (22). In the wind/solar PV only cases, the capacity factor is maximised by assigning $\gamma_n = \text{K}$ to the countries with the highest capacity factor for wind/solar PV and $\gamma_n = \frac{1}{\text{K}}$

to the remaining countries, except for a single in-between country. Examples for K = 2 are shown in figure 1. Similar to the β layouts, ν_{max} layouts for arbitrary α values can be expressed as a linear combination of the wind and solar PV only layouts.

2.4. Optimized layouts

The optimization objective is minimization of the LCOE with respect to the 60 variables $\gamma_1, ..., \gamma_N, \alpha_1, ..., \alpha_N$. A number of optimization algorithms were tested of which Cukoo Search (CS), described in appendix Appendix.1, was found to be the most successful. All optimized layouts have been obtained using the CS algorithm. They will be denoted CS layouts.

3. Results

An overview of the key variables is shown in figure 2. For backup energy and backup capacity, the optimal α value is around 0.9, which is slightly higher than the values found by [7, 8]. The difference can be attributed to the different data sets used for wind and solar PV. For transmission capacity, the minimum is around $\alpha = 0.4$, indicating a high share of solar PV. While the wind correlation length is around ≈ 1000 km [17] and thus smaller than Europe, the occurrence of sun light is highly correlated for the European countries [18]. Therefore, a high wind share causes more power to flow between the countries.

The main variable of interest, the LCOE, shows a very clear tendency. The more wind, the lower the cost. The tendency is a consequence of the significantly higher cost of energy production for solar PV compared to onshore wind. The CapEx is 50% higher and the capacity factor, on average, around 40% lower. Even though the cost of backup energy, backup capacity and transmission capacity is lowered by the introduction of a small solar component, the savings do not compensate the higher cost of production for solar PV compared to onshore wind.

The cost components for the optimal β, ν_{max} and CS layouts are shown in figure 3. From this figure it is clear that the VRES cost is dominating, which explains the wind monopole for the β and ν_{max} layouts. The CS layouts include a small solar component, decreasing with increasing K values. The CS layouts are noticeably cheaper than both the β and the ν_{max} layouts, primarily due a decrease in transmission costs.

The optimal β, ν_{max} and CS layouts are shown in figure 4. Note that for $K = 1$, the β and the ν_{max} layouts are both equal to the homogeneous layout. From figures 4b and 4c we see that the ν_{max} and the CS layouts are quite similar. These figures also explain why the CS algorithm is able to include a solar component at a competitive cost; unlike the β and ν_{max} layout definitions, the CS algorithm has the freedom to assign solar only to countries with poor

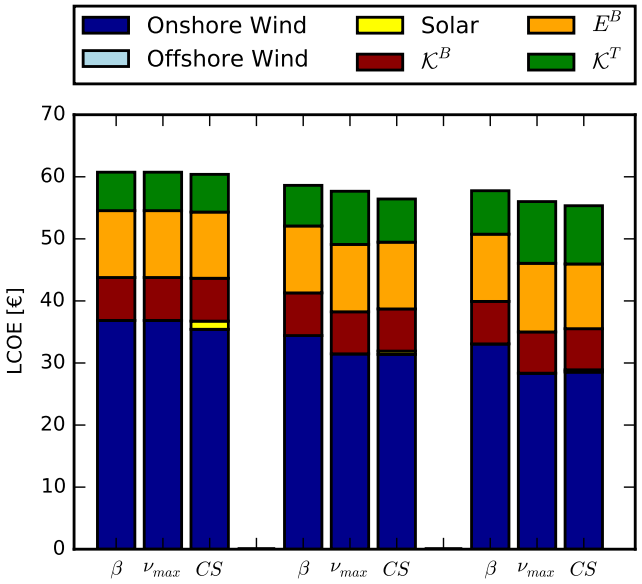

Figure 3: Cost details for the optimal β, ν_{max} and CS layouts for K = 1 (left), 2 (middle) and 3 (right).

wind resources, e.g. Serbia (RS) and Slovenia (SI). In addition, the CS algorithms reallocates some of the wind resources, e.g. from Latvia (LV) to Portugal (PT), to counteract power flows.

The β layouts are shown in (a) and the ν_{max} layouts in (b). In both cases, $\alpha = 1$ correspond to the cost optimal mix. The optimal CS layouts are shown in (c).

4. Sensitivity analysis

4.1. Excluding transmission in the optimization

While the main findings include only three optimized layouts, for K = 1, 2 and 3, numerous optimizations must be performed to allow convergence analysis, parameter tuning, and sensitivity analysis. In this case, each optimization taking more than a day is impractical.

As mentioned in appendix Appendix.1, the computation time can be decreased by analysing only a subset of the 32 years of data. However, going below one year is not ideal as this choice would imply neglecting important seasonal fluctuations. Numerically, the most costly operation in the analysis is the quadratic optimization problem, equation (10), which is solved in each iteration to determine the flows. This step is not needed to determine backup properties. By skipping the step, it is possible to speed up the optimization by more than a factor of 50. Layouts obtained by optimization excluding transmission are shown in figure 5.

It is clear that the optimization succeeds in decreasing the cost of all, but the transmission component. However, for K = 2 and K = 3, the associated increase in transmission cost is so large that the CS layouts end up being more expensive than the ν_{max} layouts at $\alpha = 1$.

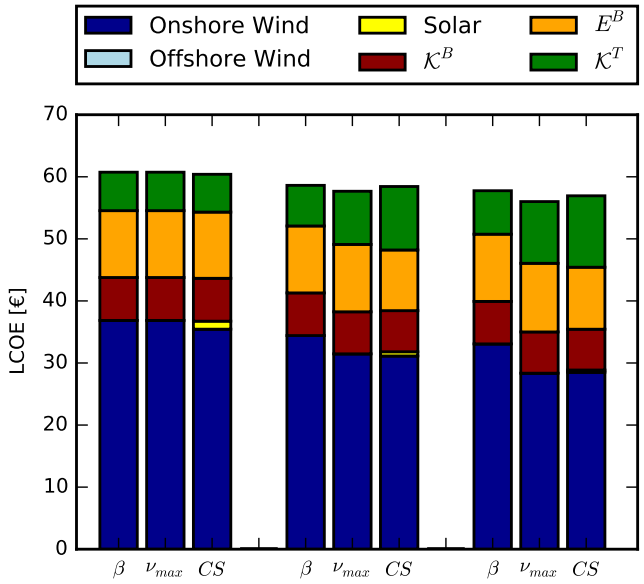

Figure 5: Cost details for the optimal layouts for K = 1 (left), 2 (middle) and 3 (right) for β, ν_{max} and CS (transmission excluded).

The difference between the CS layouts with transmission included/excluded is noticeable, but the CS solution obtained without transmission is still fairly good. For convergence analysis, parameter tuning, and sensitivity analysis, optimizations have been performed excluding transmission costs. This includes all CS solutions presented in this section.

To illustrate how the CS solution changes when transmission is taken into account, the link usage for the two solutions for K = 2 is shown in figure 6.

From figure 6 we see that in the CS layout obtained with transmission included, the resources have been reallocated in such a way that the link usage is decreased. In particular, the load on HVDC links (shown in red) is lower. Since the cost of HVDC links is significantly higher than the cost of AC links, it makes perfect sense that the load on these links has been decreased the most.

4.2. Reduced solar cost

For the β as well as the ν_{max} layouts, the optimal α values are 1. Even for the CS layouts, only a minor solar component is present. As mentioned previously, this tendency is a consequence of the higher cost of energy production for solar PV compared to onshore wind. In this section, the sensitivity of the optimum to the the solar cost is explored. In figure 7, the LCOE as a function of α is shown, similar to the lower left of figure 2, when the solar cost is reduced by a factor of 2 and 4 respectively.

A reduction of the solar cost by a factor of 2 shifts the optimal mix from 1 to around 0.9 similar to the optimum for backup energy and backup capacity. The shift indicates that the energy production cost for solar PV is becoming competitive to onshore wind. At a cost reduction of a factor of 4, the optimal mix is shifted further to around 0.7, indicating that the energy production cost for solar PV is now lower than for onshore wind. The favouring of wind even when the production cost of solar PV is lower is a consequence of the strong diurnal pattern leading to high backup requirements. The exact α values are listed in table 3.

Table 3: Alpha values for optimal layouts for different scalings of the solar cost.

(a) Cost reductions by a factor of 2.

	K = 1	K = 2	K = 3
β	0.87	0.93	0.93
ν_{max}	0.87	0.87	0.87
CS	0.82	0.92	0.93

(b) Cost reductions by a factor of 4.

	K = 1	K = 2	K = 3
β	0.67	0.67	0.67
ν_{max}	0.67	0.67	0.73
CS	0.68	0.78	0.81

4.3. Offshore wind

In the previous discussion, wind was assumed to be onshore only. By January 2014, the total European onshore wind capacity was 120.8GW, while the offshore capacity was 8.0GW [19]. While these numbers confirm the onshore-only assumption to be reasonable at present, the increasing share of offshore wind raises the question how the LCOE will be affected by the introduction of an offshore component. The immediate expectation is a significant increase in the LCOE since the cost of offshore wind is more than 100% higher compared to onshore wind due to foundation expenses along with increased maintenance costs. On the other hand, capacity factors for offshore sites are generally significantly higher than for onshore sites as indicated by table 1.

It would be possible to introduce offshore wind on equal footing with onshore wind and solar PV. However, since offshore wind is much more expensive, an optimized layout would pose a 0% offshore component, which is not a very interesting nor surprising result. Instead, a fixed offshore component is introduced by splitting the wind component into an onshore γ^W and an offshore $\tilde{\gamma}^W$ component,

$$\gamma^W \to \gamma^W + \tilde{\gamma}^W, \tag{23}$$

for countries with suitable offshore regions. Explicitly these are: Denmark, Germany, Great Britain, Ireland, the Netherlands, France, Belgium, Norway and Sweden. Other countries retain onshore wind only. The magnitude of the offshore component is assigned by requiring that the

offshore wind power generation accounts for a fixed share of the total wind power generation,

$$\text{offshore share} = \frac{\tilde{\gamma}^W}{\gamma^W + \tilde{\gamma}^W}. \tag{24}$$

Cost details for optimized layouts with fixed offshore shares of 0%, 25% and 50% are shown in figure 8.

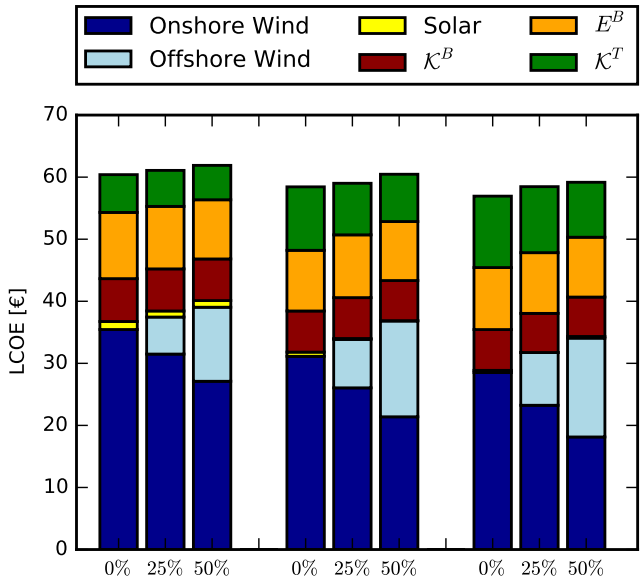

Figure 8: Cost details for the CS optimal layouts for K = 1 (left), 2 (middle) and 3 (right) for offshore shares of 0%, 25% and 50%.

From figure 8 it is clear that the introduction of an offshore component increases the LCOE. However, the increase in LCOE is not dramatic. While the cost of wind energy increases significantly, the cost of backup and transmission decreases slightly. The decrease is a consequence of the difference in the temporal production pattern from onshore to offshore wind. In some time steps the onshore production is low while the offshore production is high. The introduction of an offshore component thus tends to smooth out the wind production time series. As a side effect, solar becomes less favourable as illustrated by figure 8. The CS optimized layouts for an offshore share of 50% are shown in figure 9.

5. Discussion and conclusions

The dependence on the layout of VRES of a number of key parameters along with the resulting LCOE has been investigated. It was found that the backup and transmission costs are significant, but main costs are associated with the VRES capacities. The VRES capacity costs can be lowered by allocating more resources to countries with high capacity factors. At a heterogeneity factor of $K = 2$, meaning that each country installs VRES capacities covering a minimum of 50% and maximum of 200% of their mean load, the LCOE can be lowered by almost 5% by choosing the heuristic ν_{max} layout which maximises the overall capacity factor. Further reduction of the cost can be achieved by reducing backup and/or transmission costs. Using the cuckoo search algorithm, such a layout was found to reduce the LCOE by an additional 2%. While the additional cost reduction of 2% relies heavily on the current network structure, the primary cost reduction is of a more general nature. It can be attributed to the general tendency for the heterogeneous layouts to move wind capacities towards the North Sea countries. Since the wind resource quality is better than for the central and southern countries, the reallocation results in lower costs.

The cost optimal layouts considered in the main analysis are almost exclusively based on onshore wind. The reason is that onshore wind is significantly cheaper than solar, partly due to lower capital expenses, partly due to lower capacity factor. It was found that the cost of solar must decrease by a factor of ≈ 2 for a significant solar component to become profitable. Besides lowering the capital expenses, the solar cost could also be lowered by increasing the capacity factor. Based on data from [6], the capacity factor can be increased by $\approx 40\%$ by applying dual axis tracking compared to the fixed position installation assumed in table 1. In addition, studies on increasing the energy conversion efficiency are still being conducted.

The main analysis considered onshore wind only, but the effect of introducing an offshore component was also discussed. Foundation expenses and increased maintenance costs makes offshore wind significantly more expensive than onshore wind. Some of the additional expenses are compensated by higher offshore capacity factors along with a more stable temporal production pattern, but at the end of the day, offshore wind is still more expensive than onshore wind. However, there are other incentives for offshore wind. The opposition from residents is usually lower than for onshore wind, and the potential for expansion larger. The number of suitable onshore sites are final, and when they are exhausted, offshore wind might be the best alternative.

In conclusion, it was found that a heterogeneous layout with wind resources shifted towards the North Sea countries decreases the LCOE by around 5% compared to the homogeneous layout at the optimal mix. An additional reduction by 2% was possible by taking also transmission and backup costs into account.

The effect of integrating one or more storage elements in the electricity system has not been considered in this paper. Promising storage projects are already in the making, so by the time Europe reaches $\gamma = 1$, commercial large scale storage systems are presumably available. A natural extension of this paper would be to include various types of storage.

Table 1: Capacity factors ν_n^w, $\tilde{\nu}_n^w$ and ν_n^s for onshore wind, offshore wind and solar PV for the European countries.

	ν_n^w	$\tilde{\nu}_n^w$	ν_n^s		ν_n^w	$\tilde{\nu}_n^w$	ν_n^s		ν_n^w	$\tilde{\nu}_n^w$	ν_n^s
AT	0.16	-	0.15	DE	0.26	0.53	0.13	NO	0.31	0.44	0.12
BE	0.27	0.49	0.12	GB	0.39	0.53	0.11	PL	0.22	0.42	0.13
BA	0.16	-	0.16	GR	0.17	0.43	0.17	PT	0.23	0.25	0.18
BG	0.14	0.24	0.17	HU	0.14	-	0.15	RO	0.13	0.31	0.16
HR	0.21	0.28	0.16	IE	0.43	0.47	0.10	RS	0.11	-	0.16
CZ	0.19	-	0.14	IT	0.17	0.21	0.17	SK	0.15	-	0.15
DK	0.45	0.54	0.12	LV	0.29	0.42	0.11	SI	0.09	-	0.15
EE	0.33	0.41	0.11	LT	0.25	0.40	0.11	ES	0.19	0.26	0.18
FI	0.23	0.41	0.10	LU	0.24	-	0.13	SE	0.26	0.41	0.12
FR	0.25	0.42	0.15	NL	0.34	0.53	0.12	CH	0.16	-	0.16

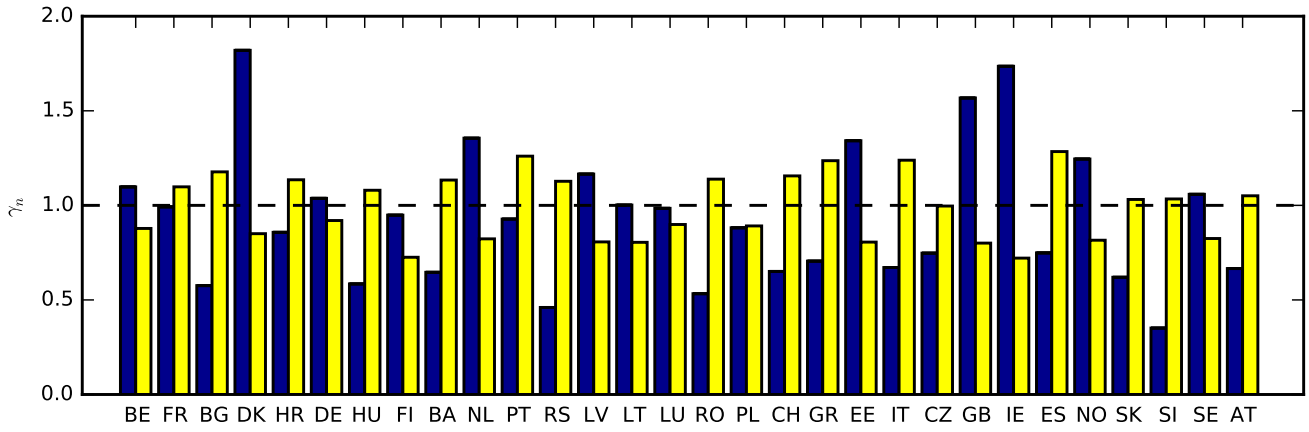

(a) Examples of β layouts for $\beta = 1$.

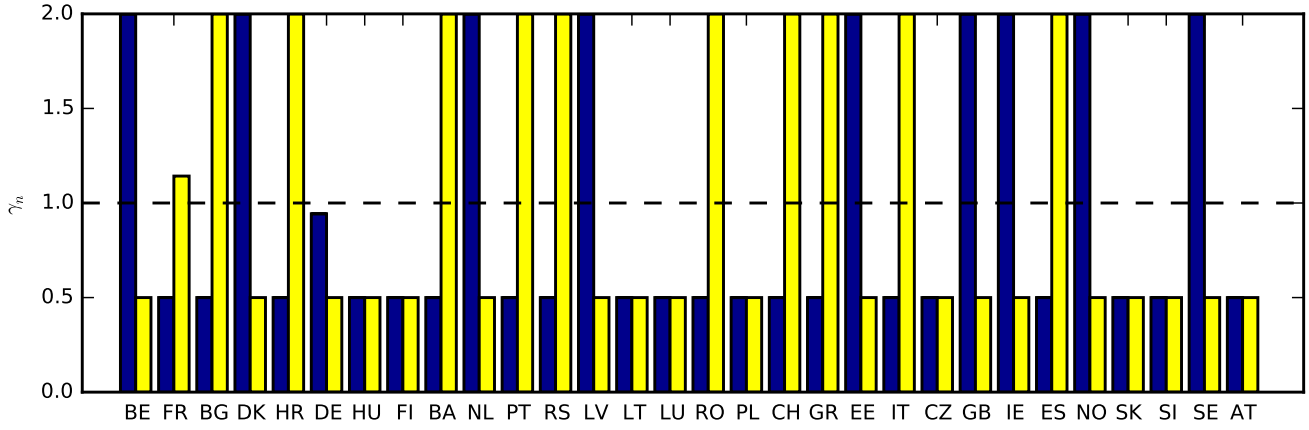

(b) Examples of ν_{max} layouts constrained by K = 2 .

Figure 1: Examples of heuristic layouts. In each sub figure, two sets of bars corresponding to the $\alpha = 1$ and the $\alpha = 0$ layouts respectively are shown.

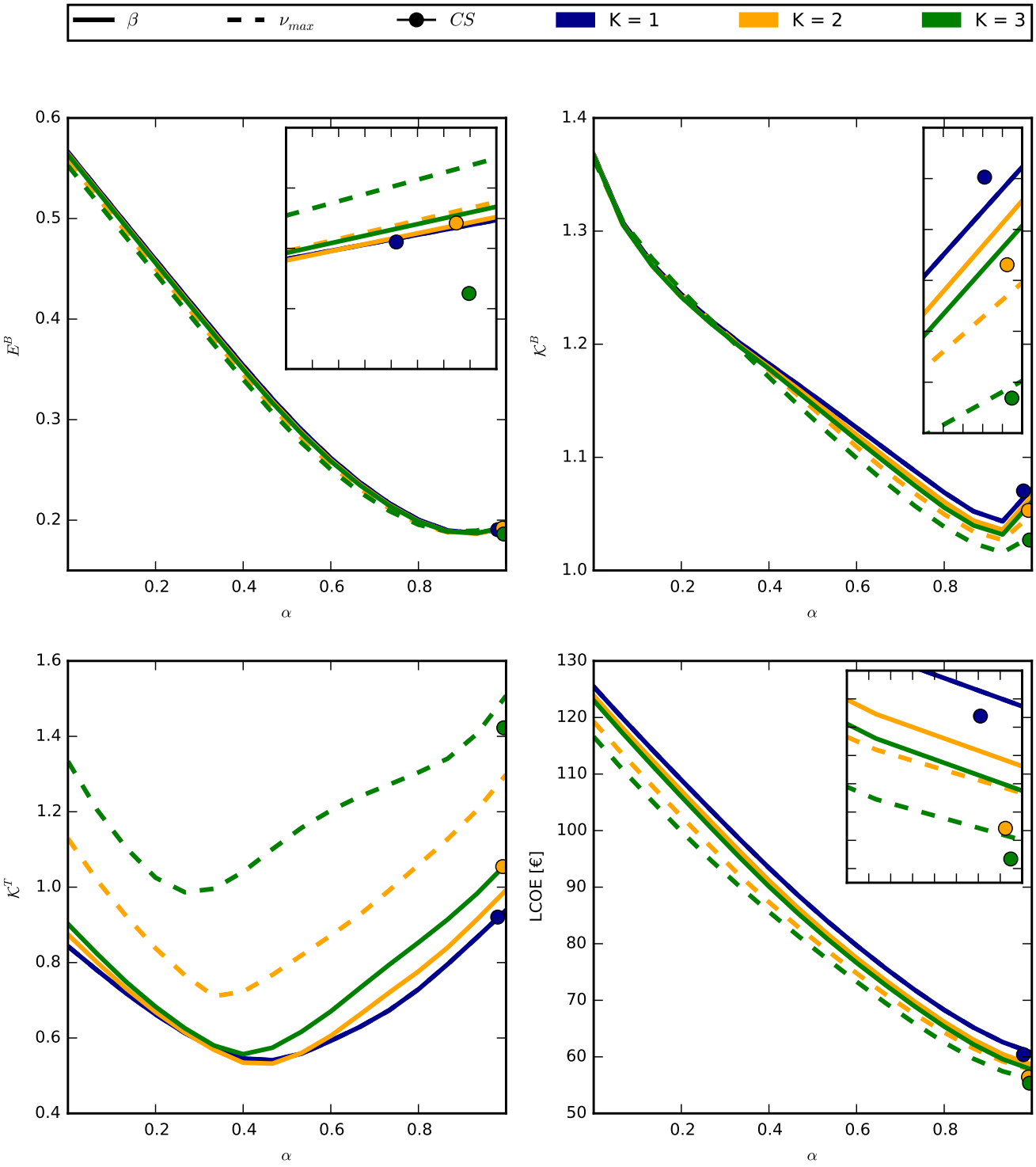

Figure 2: Overview of the key variables, backup energy E^B, backup capacity $\mathcal{K}^B$ and transmission capacity $\mathcal{K}^T$ along with the associated LCOE.

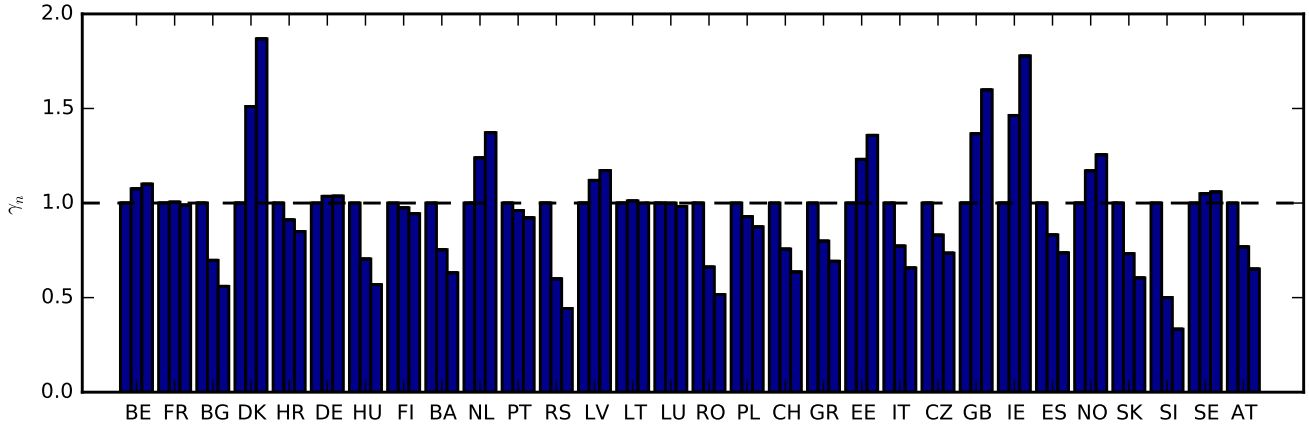

(a) Optimal β layouts (optimal mix at $\alpha = 1$).

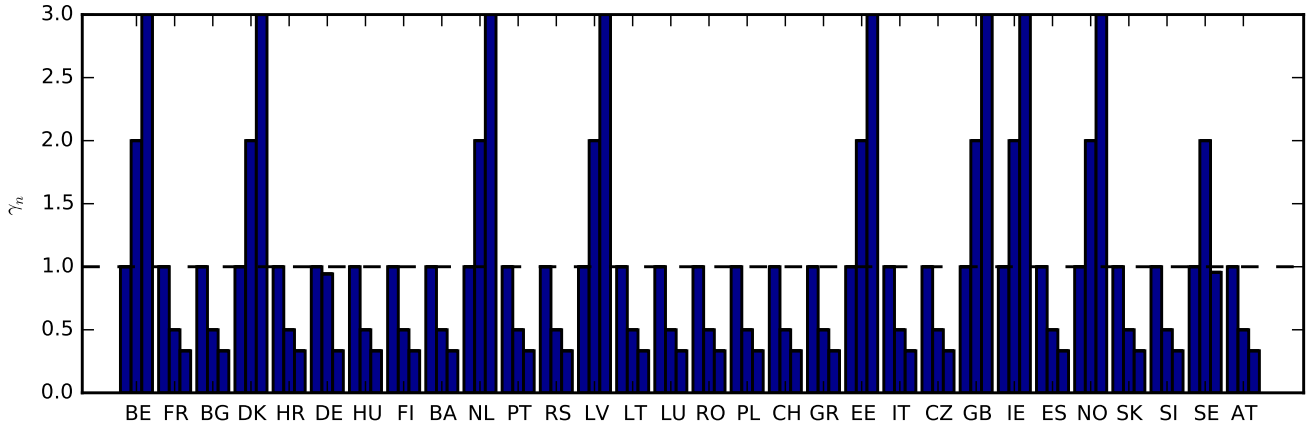

(b) Optimal ν_{max} layouts (optimal mix at $\alpha = 1$).

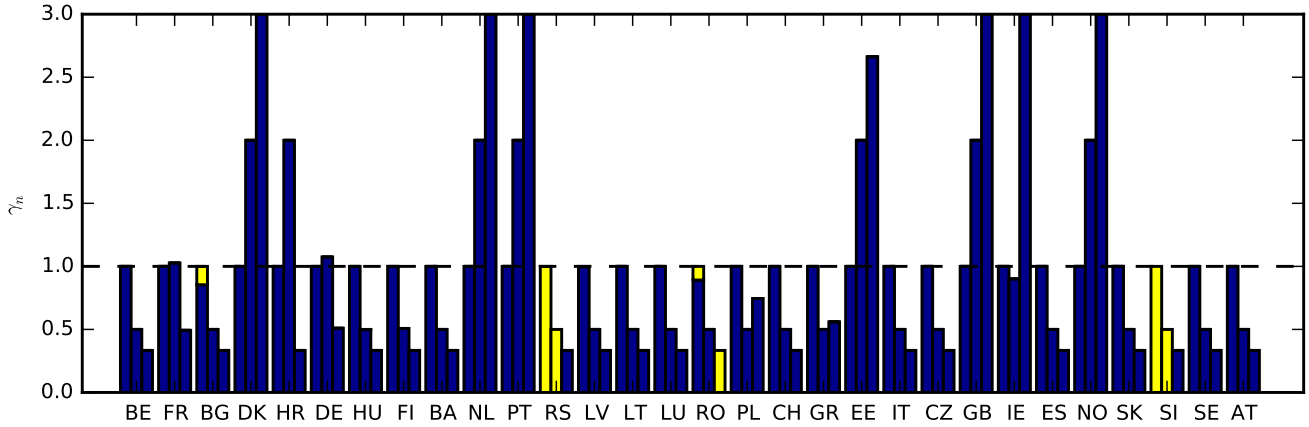

(c) CS optimized layouts.

Figure 4: Optimal layouts. In each sub figure, three sets of bars corresponding to values of K = 1 (left), 2 (middle), and 3 (right) are shown.

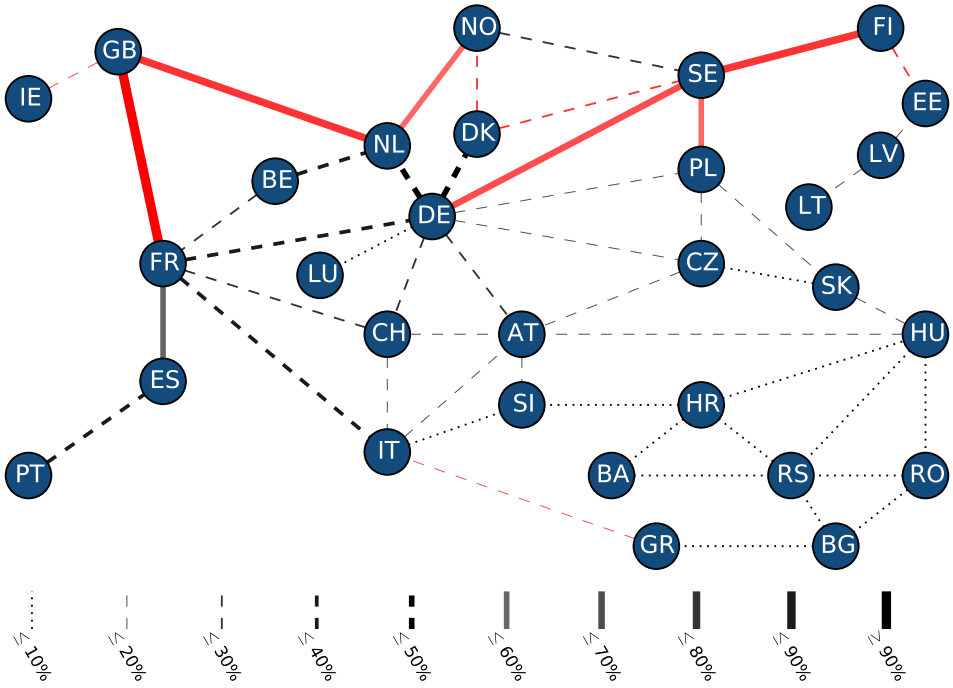

(a) Link usage for the CS layout (transmission excluded) constrained by K = 2.

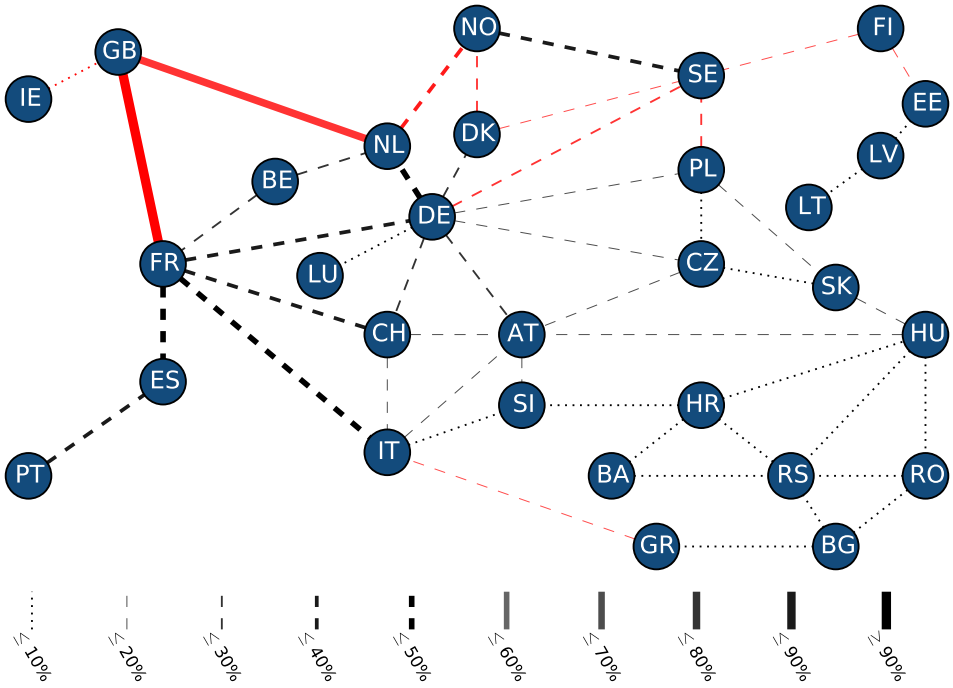

(b) Link usage for the CS layout (transmission included) constrained by K = 2.

Figure 6: Overview of link usage. AC links are shown in black while HVDC links are shown in red. Link capacities are indicated relative to the highest flow (74 GW between Great Britain and France in figure 6a). As transmission costs are included in the optimization, the layout is altered in a way that tends to decrease the load on HVDC links. This tendency can be attributed to the fact that the cost of HVDC links is significantly higher than the cost of AC links. An exception is Great Britain where ν^W is so high that the resulting low cost of wind energy outweighs the cost of the HVDC connections.

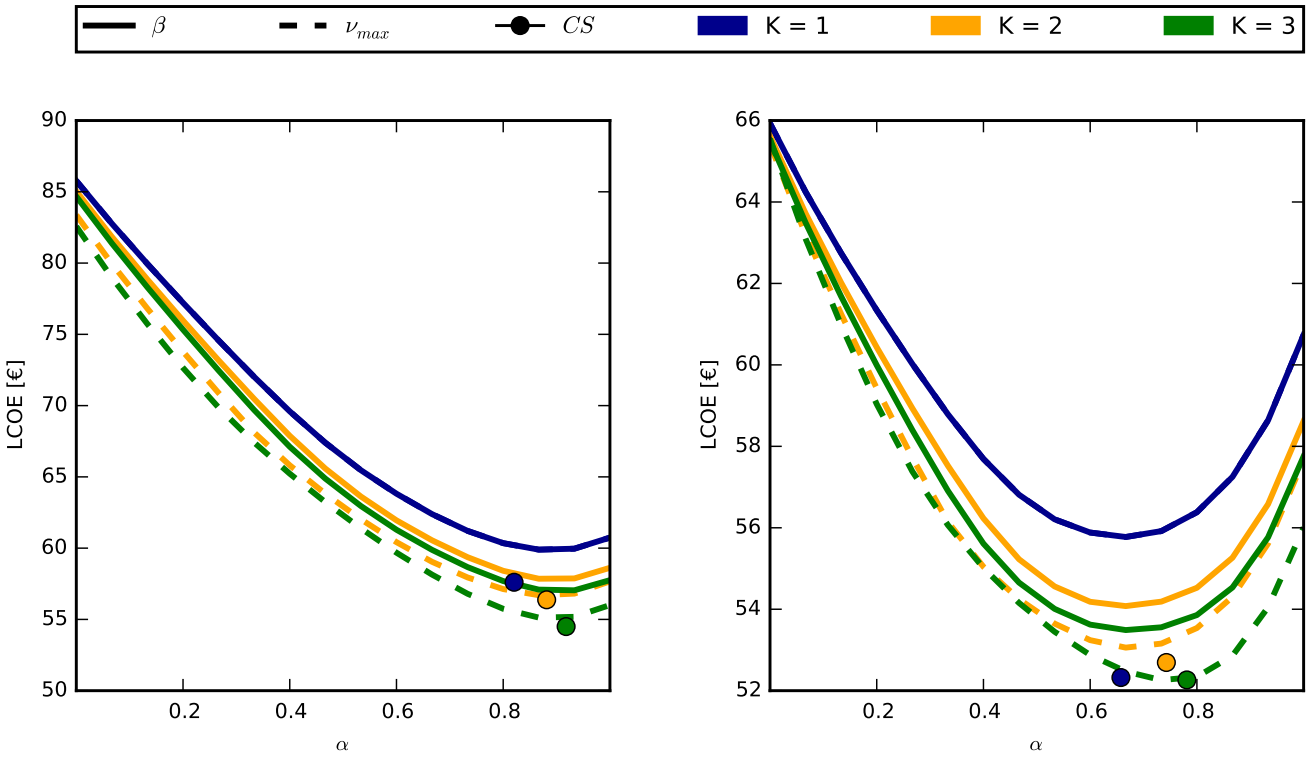

Figure 7: LCOE for different scalings of the solar cost. Shown are cost reductions by a factor of 2 (left) and 4 (right). From the figure, it is clear that for solar PV to be cost competitive to onshore wind, the cost must drop by a factor of ≈ 2.

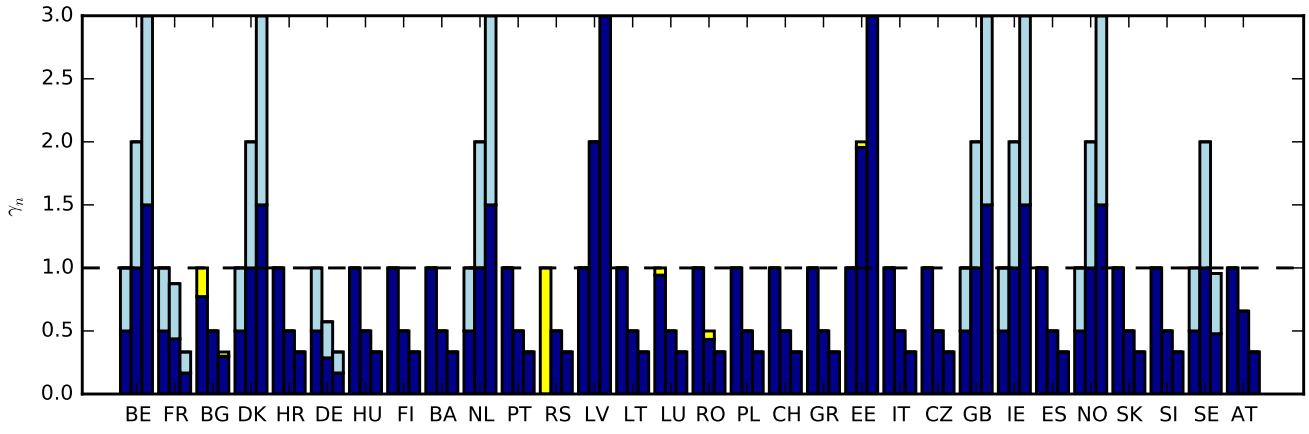

Figure 9: CS layouts constrained by K = 1 (left), 2 (middle) and 3 (right) for an offshore share of 50% for Denmark, Germany, Great Britain, Ireland, Netherlands, France, Belgium, Norway and Sweden.

Bibliography

[1] European Commission. A roadmap for moving to a competitive low carbon economy in 2050. Technical report, EC, March 2011.

[2] James H. Williams, Andrew DeBenedictis, Rebecca Ghanadan, Amber Mahone, Jack Moore, William R. Morrow, Snuller Price, and Margaret S. Torn. The Technology Path to Deep Greenhouse Gas Emissions Cuts by 2050: The Pivotal Role of Electricity. Science, 335:53–59, 2012. http://dx.doi.org/10.1126/science.1208365.

[3] McKinsey & Company, KEMA, The Energy Futures Lab at Imperial College London, Oxford Economics, and ECF. Roadmap 2050 – A practical guide to a prosperous, low-carbon Europe. Technical report, European Climate Foundation, http://www.roadmap2050.eu/, April 2010. Online, accessed June 2012.

[4] Rolando A. Rodriguez, Sarah Becker, Gorm Bruun Andresen, Dominik Heide, and Martin Greiner. Transmission needs across a fully renewable European power system. Renewable Energy, 63:467–476, March 2014.

[5] Sarah Becker, Rolando A. Rodríguez, Gorm B. Andresen, Stefan Schramm, and Martin Greiner. Transmission grid extensions during the build-up of a fully renewable pan-European electricity supply. Energy, 64:404–418, January 2014.

[6] Gorm Bruun Andresen, Anders Aspegren Søndergaard, and Martin Greiner. Validation of danish wind time series from a new global renewable energy atlas for energy system analysis. Elsevier, 2014.

[7] Heide, D., von Bremen, L., Greiner, M., Hoffmann, C., Speckmann, M., and Bofinger, S. Seasonal optimal mix of wind and solar power in a future, highly renewable Europe. Renewable Energy, 35(11):2483–2489, 2010.

[8] Heide, D., Greiner, M., Von Bremen, L., and Hoffmann, C. Reduced storage and balancing needs in a fully renewable European power system with excess wind and solar power generation. Renewable Energy, 36(9):2515–2523, 2011.

[9] Magnus Dahl. Power-flow modeling in complex renewable electricity networks. Master's thesis, Aarhus University, 2015.

[10] Rodriguez, R.A., Becker, S., and Greiner, M. Cost-optimal design of a simplified, highly renewable pan-European electricity system. 2014.

[11] Rolando A. Rodriguez. Weather driven power transmission in a highly renewable European electricity network. PhD thesis, Aarhus University, 2014.

[12] Kost, C., Schlegl, T., Thomsen, J., Nold, S., and Mayer, J. Levelized cost of electricity: renewable energies. Technical report, Fraunhofer Institute for solar energy systems ISE, 2012. Online, retrieved October 2013.

[13] McKinsey. RoadMap 2050: A Practical Guide to a Prosperous, Low-Carbon Europe. Technical report, European Climate Foundation, 2010. Online, retrieved October 2013.

[14] Schaber, K., Steinke, F., and Hamacher, T. Transmission grid extensions for the integration of variable renewable energies in Europe: Who benefits where? Energy Policy, 43:123 – 135, 2012.

[15] Schaber, K., Steinke, F., Mühlich, P., and Hamacher, T. Parametric study of variable renewable energy integration in Europe: Advantages and costs of transmission grid extensions. Energy Policy, 42:498–508, 2012.

[16] W. Short, D. Packey, and T. Holt. A manual for the economic evalua- tion of energy efficiency and renewable energy technologies. Technical report, National Renewable Energy Laboratory, 1995.

[17] J. Widen. Correlations between large-scale solar and wind power in a future scenario for sweden. IEEE Transactions on Sustainable Energy, 2(2):177–184, 2011.

[18] Timo Zeyer. Modeling of spatio-temporal flow patterns in a fully renewable pan-european power system. Master's thesis, Aarhus University, 2013.

[19] G. Corbetta, I. Pineda, and J. Wilkes. Wind in power 2014 european statistics. Technical report, The European Wind Association, 2015.

[20] David E. Goldberg. Genetic Algorithms in Search, Optimization and Machine Learning. Addison-Wesley Longman Publishing Co., Inc., Boston, MA, USA, 1st edition, 1989.

[21] J. Kennedy and R. Eberhart. Particle swarm optimization. In Neural Networks, 1995. Proceedings., IEEE International Conference on, volume 4, pages 1942–1948 vol.4. IEEE, November 1995.

[22] Xin-She Yang and Suash Deb. Cuckoo search via lévy flights. In NaBIC, pages 210–214. IEEE, 2009.

[23] R. B. Payne. The Cuckoos. Oxford University Press, 2005.

[24] S. Walton, O. Hassan, K. Morgan, and M.R. Brown. Modified cuckoo search: A new gradient free optimisation algorithm. Chaos, Solitons & Fractals, 44(9):710 – 718, 2011.

[25] Milan Tuba, Milos Subotic, and Nadezda Stanarevic. Modified cuckoo search algorithm for unconstrained optimization problems. In Proceedings of the 5th European Conference on European Computing Conference, ECC'11, pages 263–268, Stevens Point, Wisconsin, USA, 2011. World Scientific and Engineering Academy and Society (WSEAS).

[26] Andy M. Reynolds and Mark A. Frye. Free-flight odor tracking in drosophila is consistent with an optimal intermittent scale-free search. PLoS ONE, 2(4):e354, 04 2007.

[27] Aleksander Janicki and Aleksander Weron. Simulation and Chaotic Behavior of Alpha-stable Stochastic Processes. Number hsbook9401 in HSC Books. Hugo Steinhaus Center, Wroclaw University of Technology, 1994.

Appendix.1. Cuckoo search

For notational convenience, a complete layout vector $\boldsymbol{x}$ is constructed as $x_1 = \gamma_1, ..., x_N = \gamma_N, x_{N+1} = \alpha_1, ..., x_{2N} = \alpha_N$. The optimization objective is global minimization of the LCOE as a function of $\boldsymbol{x}$. The LCOE is a complicated function of the layout $\boldsymbol{x}$ for which derivative information is not available. With 30 countries, the dimensionality of the problem is 60, and the search space thus large.

Efficient global optimization within a large search space is a problem which has been successfully addressed by a number of Nature inspired meta heuristic algorithms. By imitating the best features in nature, these algorithms achieve a unique balance between intensification (search around the current best solution[1]) and diversification (exploration of the search space). Typical examples are genetic algorithms [20] and particle swarm optimization [21]. In this paper, a recent addition [22] to the family, cuckoo search (CS), has been applied.

Cuckoo birds practice an aggressive breeding behaviour where the female cuckoos lay their eggs in the nests of other birds. If the host bird discovers the alien egg, the egg is thrown away, or the nest is abandoned. To avoid this fate, some cuckoo species have specialized in mimicking the visual appearance of the egg of the host species [23]. In the CS algorithm, the cuckoo eggs represent solutions. The nest is simply a container holding one or more eggs. For simplicity, each nest will hold only one egg. The actual implementation differs slightly across the literature[22, 24, 25], but most implementations follow a common structure:

1. Initially, each of the X nests are populated by an egg selected randomly from within the solution space.
2. A fraction p of the eggs are discovered by the host bird and abandoned.
3. New eggs are generated and dropped into the nests. The receiving nest rejects the worse of the two eggs.
4. Step 2 and 3 are repeated until a user defined termination criteria is fulfilled.

Inspired by the flight pattern of fruit flies[26], new eggs are generated by Lévy flights. A Lévy flight is a random walk with the Markov property. The step size is drawn from a Lévy α-stable distributionwith scale parameter $c = 1$, location parameter $\mu = 0$, stability parameter $\alpha = 1/2$ and skewness parameter $\beta = 1$. The large tail causes occasional jumps ensuring efficient diversification. The Lévy distribution was generated using a general method for generation of Lévy α-stable distributions[27].

In the CS implementation used in this paper, the eggs are split into bad eggs (the to-be-abandoned p fraction) and good eggs (the remaining $1 - p$ fraction). The bad eggs are replaced immediately by new ones generated by Lévy flights starting from the old eggs. New trails eggs are generated by Lévy flights starting from the good eggs. Each trail egg is dropped into a random nest, and the receiving nest rejects the worse of the two eggs. A value of p around 0.75 gave the best performance. Mimicking of the host egg, approximated by the current best egg $\boldsymbol{x}_{best}$, is modelled by biasing the Lévy flight towards $\boldsymbol{x}_{best}$. In practice, the step size is scaled by a factor of $(\boldsymbol{x}_{best} - \boldsymbol{x}_i)$. The Lévy flight thus takes the form

$$\boldsymbol{x} \to \boldsymbol{x} + A\,(\boldsymbol{x}_{best} - \boldsymbol{x})\,\text{Lévy}(z) \tag{.1}$$

where A denotes a problem specific scaling parameter. For most problems (the current included), a value $A \approx 1$ is appropriate. It is possible that a solution generated by Lévy flight is outside the search space defined by equation (22) and the implicit constraint $0 \leq \alpha_n \leq 1$. In this case, any invalid value is shifted to the nearest boundary value: A value of $\alpha_n = 1.1$ is changed to $\alpha_n = 1.0$ while a value of $\gamma_n = \frac{1}{K+2}$ is changed to $\gamma_n = \frac{1}{K}$.

When a solution is generated, the solution is renormalized by a linear scaling of the γ values such that

$$\sum_n \gamma_n \langle L_n \rangle = \langle L_{EU} \rangle \tag{.2}$$

is fulfilled. The renormalization might cause a violation of equation (22). In this case, the solution is rejected and a new one generated. This procedure is repeated until a valid solution is found.

The termination criteria was chosen as a fixed number of iterations. In each iteration, X function evaluations are performed, each requiring a loop through the 32 year dataset solving a quadratic optimization problem at each time step. Therefore, a single function evaluation takes around 15 minutes on a standard laptop anno 2015. To decrease computation time, a single model year was used rather than the full 32 year data set.

Starting from a completely random population, it was found that around 50,000 function evaluations were required to reach a stable solution[2]. It is possible to decrease the required number of function evaluations by planting a best-guess solution in the initial population. The drawback of this approach is the biasing of the search. Other, potentially better, solutions are less likely to be found due to the initial biasing. Starting from random populations, the stable points obtained for K = 1, 2, 3 were all found to be very similar to the ν_{max} solutions. This indicates that the ν_{max} solution is probably close to the global optimum. Therefore, the final optimizations have been performed biased by the ν_{max} solution effectively decreasing the number of required function evaluations by almost an order of magnitude. With these approximations, the computation time is decreased from ≈ 1.5 years to less than two days.

For the problem at hand, the performance of the CS algorithm turned out to be relatively insensitive to changes

[1] In this section, the terms *layout* and *solution* are used interchangeably.

[2] Non-biased optimizations and parameter tuning were performed excluding transmission costs to decrease computation time, see section 4.1 for details.

Algorithm 1 Pseudo code for the cuckoo search implementation. The *Evaluate* function evaluates egg costs. By passing an array of eggs to the *Evaluate* function, rather than evaluation the eggs one by one, parallel evaluation is possible. The *Sort* function sorts the eggs by cost in ascending order.

```
function CuckooSearch
    nests ← X eggs selected randomly from within the solution space
    Evaluate(nests)
    Sort(nests)
    bestNest ← nests[0]
    generation ← 0
    while termination criteria not fulfilled do
        for index i of bad nests do
            nests[i]← levy flight starting from nests[i]
        for index i of good nests do
            trailEggs[i]← levy flight starting from nests[i]
        Evaluate(nests)
        Evaluate(trailEggs)
        for index i of trailEggs do
            j ← index of a random nest
            if cost of nest[j] > cost of trailEggs[i] then
                nest[j] ← trailEggs[i]
        Sort(nests)
        bestNest ← nests[0]
        generation ← generation + 1
    return bestNest
```

in A, p and X. Values of A between 1 and 50 resulted in similar performance, while larger values of A caused a drop in performance, probably due to the average step size becoming too large. Likewise, values of p between 0.65 and 0.85 resulted in similar performance, while values outside this interval caused drops in performance. For X, the best performance was observed around a value of 50. Values below 25 and above 100 caused the algorithm to get stuck in local minima.